A Momentum-Based Modeling of Jet-Induced Sealing Flow

[Author Name]

Abstract

We present a steady, incompressible and axisymmetric model for jet-induced sealing in thin gaps. The formulation is derived directly from local and global conservation of mass and momentum in three coupled regions: the confined core, the vertical jet, and the radial wall-jet after impact. No interface tuning is introduced; the sealing pressure, jet deflection, leakage and lift emerge from the balance equations closed with measurable correlations (e.g. wall shear in the wall-jet). We provide a rigorous description of the system geometry, operating principle and objectives, the governing equations and interface conditions, and a complete description of the numerical solver with pseudocode.

1 Introduction

High-speed jets impinging on confined gaps can generate pressure distributions capable of sustaining external loads and reducing leakage. This mechanism, here termed *jet-induced sealing*, originates from the redistribution of momentum between the incoming jet, the confined core flow, and the wall-jet along the adjacent surface. A physically consistent description must *derive* sealing pressures and leakage from the dynamic equilibrium of the flow.

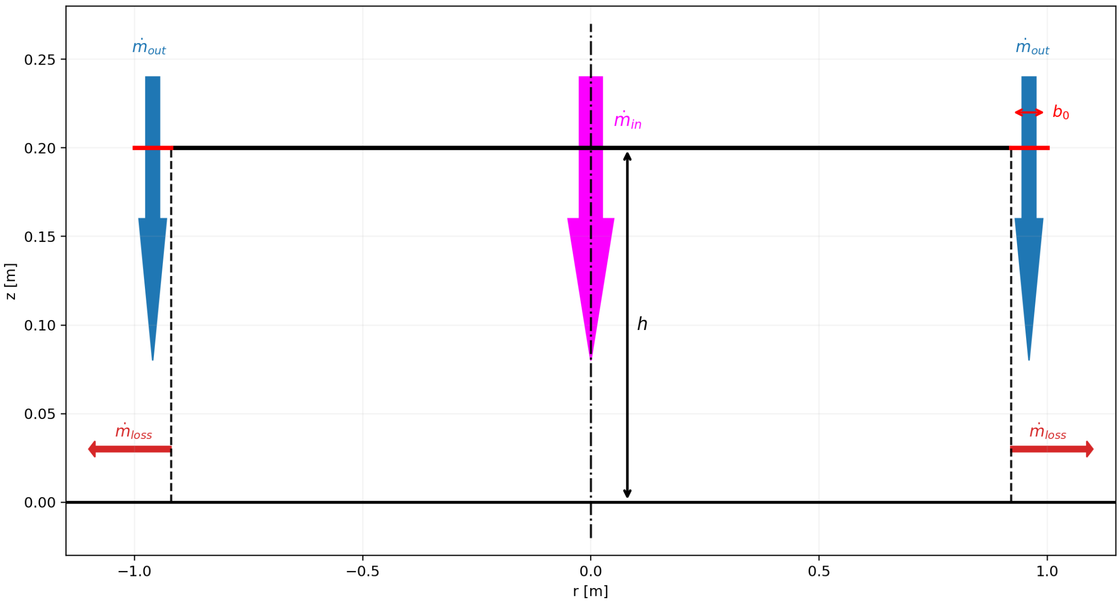

Figure 1 – Schematic of the hovering disc with two concentric jets: the outer annular curtain and the central make-up flow.

2 System Description and Objectives

Geometry and flow layout. We consider two horizontal surfaces separated by a nominal gap h with $h \ll R$, where R is the characteristic radial extent. An annular slot of width b_0

at radius R^- injects a vertical jet of density ρ and mean speed U_j directed towards the base surface. Upon impingement, the jet turns into a radial wall-jet of thickness $\delta(r)$ along the base. The confined *core* occupies $0 \le r \le R^-$ within the gap.

Operating principle. The vertical momentum of the jet is partially converted into pressure in a narrow turning region near $r \approx r_t \lesssim R^-$, creating a pedestal overpressure $p_{\text{ped}}(r)$ which raises the core pressure p_c and reduces leakage. The resulting pressure field produces a lift $L = \int_0^{R^-} (p_c - p_0)\, 2\pi r\, dr$ that can support an external load W while keeping leakage $\dot{m}_{\text{leak}}$ acceptably low.

Objectives. Given (h, R, b_0), fluid properties (ρ, μ) and a load W, we seek the unknowns

$$p_c(r),\ \bar{u}(r),\ U_j\ (\text{or } \dot{m}_j),\ U_w(r),\ \delta(r),\ p_{\text{ped}}(r),\ r_t,\ \dot{m}_{\text{leak}},$$

together with performance metrics (lift–height map $L(h)$, required jet power $\dot{W}_{\text{jet}}$, sealing and leakage indices, and efficiency η).

3 Physical Model

The flow is modeled as steady, axisymmetric and incompressible (air at low Mach). Three coupled regions are considered: (i) the *core* thin film in $0 \le r \le R^-$; (ii) the *vertical jet* issuing from the slot and impinging on the base; (iii) the *radial wall-jet* after turning. Coupling follows from continuity of mass and momentum.

3.1 Core (thin-film / lubrication)

Depth-averaging Navier–Stokes in the limit $h \ll R$ yields

$$\bar{u}(r) = -\frac{h^2}{12\mu}\frac{dp_c}{dr}, \qquad \frac{1}{r}\frac{d}{dr}(r\,\rho\,h\,\bar{u}) = s(r), \tag{1}$$

where $s(r)$ accounts for any distributed sources (typically $s = 0$ away from the jet). Eliminating $\bar{u}$,

$$\frac{1}{r}\frac{d}{dr}\left(-r\,\frac{\rho h^3}{12\mu}\frac{dp_c}{dr}\right) = s(r). \tag{2}$$

Boundary conditions: symmetry at $r = 0$ ($dp_c/dr = 0$) and an *unknown* edge pressure $p_c(R^-)$ provided by the turning region. The lift must balance the applied load:

$$L = \int_0^{R^-} (p_c - p_0)\, 2\pi r\, dr = W. \tag{3}$$

3.2 Jet and turning region

Let $\dot{m}_j = \rho U_j b_0$ be the jet mass flow per unit circumference. A vertical momentum balance over a control volume from the slot to the base gives

$$\dot{m}_j U_j = \int_{r_t^-}^{r_t^+} \left[p_{\text{ped}}(r) - p_0\right]\, dr + \Delta\mathcal{M}_z, \tag{4}$$

where $\Delta\mathcal{M}_z$ accounts for viscous loss and three-dimensional turning; it is not prescribed but determined implicitly by consistency with the wall-jet momentum (next subsection). The initiation of the wall-jet at r_t obeys flux continuity:

$$q(r_t) = \frac{\dot{m}_j}{2\pi r_t \rho}, \qquad m(r_t) = \frac{\dot{m}_j U_j}{2\pi r_t}. \tag{5}$$

3.3 Radial wall-jet

An integral formulation for the wall-jet of thickness $\delta(r)$ and characteristic speed $U_w(r)$ is adopted. Define $q \equiv \int_0^\delta u_r\,dz \simeq U_w\delta$ and $m \equiv \int_0^\delta \rho u_r^2\,dz \simeq \rho U_w^2\delta$. Then

$$\frac{d}{dr}(\rho q) = 2\pi r\,\rho\,E\,U_w, \tag{6}$$

$$\frac{d}{dr}(\rho m) = -\,\tau_w\,2\pi r - \frac{dp}{dr}\,2\pi r\,\delta, \tag{7}$$

where $\tau_w = \frac{1}{2}\rho C_f U_w^2$ and $E \geq 0$ admits entrainment from the surrounding fluid when relevant. Close to the wall-jet inception, $p \approx p_0$ except within the narrow turning region where $p = p_{\text{ped}}$. Standard smooth-wall correlations provide $C_f = C_f(\text{Re}_\delta)$ and a growth law $d\delta/dr$; the model is insensitive to the particular choice as long as it is physically consistent and measured.

3.4 Interface and global mass balance

The edge pressure of the core equals the local pressure at the turning rim:

$$p_c(R^-) = p_0 + p_{\text{ped}}(R^-). \tag{8}$$

The leakage through the core rim follows from (1):

$$\dot{m}_{\text{leak}} = 2\pi R^-\,\rho\,h\,\bar{u}(R^-) = -\,\frac{\pi\rho h^3}{6\mu}\,R^-\,\left.\frac{dp_c}{dr}\right|_{R^-}. \tag{9}$$

Global mass conservation relates inlet, jet and leakage:

$$\dot{m}_{\text{in}} = \dot{m}_j + \dot{m}_{\text{leak}}. \tag{10}$$

4 Non-dimensionalization (for analysis and scaling)

Let $r^* = r/R^-$, $p^* = (p - p_0)/(\rho U_j^2)$, $u^* = \bar{u}/U_j$, $\delta^* = \delta/b_0$ and define $\lambda = h/b_0 \ll 1$ and $\text{Re}_j = U_j b_0/\nu$. Equations (2)–(10) reduce to a compact set revealing the dominance of thin-film resistance and the wall-jet friction in setting $p_c(R^-)$; the seal and leakage indices follow as

$$\Pi_{\text{seal}} = \frac{\rho U_j^2 b_0}{h\,\overline{p_c}}, \qquad \Pi_{\text{leak}} = \frac{\dot{m}_{\text{leak}}}{\rho U_j\,2\pi R^- b_0}, \tag{11}$$

useful for design comparisons at fixed geometry.

5 Numerical Implementation

We solve the coupled problem by iterating between the core (thin-film ODE), the turning region momentum closure and the wall-jet integral equations until mass and lift equilibria are simultaneously satisfied. All steps are steady; no time marching is required.

Discretization. The core radius $[0, R^-]$ is discretized on a collocated grid r_i $(i = 0, \ldots, N)$ refined near R^-. Equation (2) is integrated in conservative finite-volume form with second-order central differences for dp_c/dr and boundary conditions $dp_c/dr|_{r_0} = 0$, $p_c(r_N) = p_{\text{edge}}$. The wall-jet ODE system (6)–(7) plus a growth law for δ is advanced from r_t to an outer radius $R_{\max}$ using an explicit strong-stability-preserving Runge–Kutta scheme; the initial conditions at r_t are given by (5).

Coupling and unknowns. Primary unknowns are $\{p_c(r_i)\}$, p_{edge}, $\dot{m}_j$ (or U_j), and the wall-jet fields $\{q(r), m(r), \delta(r)\}$ for $r \geq r_t$. At each nonlinear iteration we enforce: (i) edge pressure consistency (8), (ii) global mass (10), and (iii) lift balance (3).

Convergence criteria. We require the residuals

$$\mathcal{R}_p = p_{\text{edge}} - (p_0 + p_{\text{ped}}(R^-)),$$
$$\mathcal{R}_m = \dot{m}_{\text{in}} - (\dot{m}_j + \dot{m}_{\text{leak}}),$$
$$\mathcal{R}_L = L - W$$

to satisfy $|\mathcal{R}_\bullet| \leq \varepsilon_\bullet$ with tolerances $\varepsilon_p, \varepsilon_m, \varepsilon_L$ typically set to 10^{-5} in normalized units.

Algorithm (pseudocode). The following high-level pseudocode outlines the complete solver.

Listing 1 – Nonlinear solver for the coupled jet-induced sealing model.

```
Given geometry (R_minus, b0, h), fluid (rho, mu), load W, inlet m_in
Choose grid r[0..N] on [0, R_minus] (refined near R_minus)
Initialize guesses: Uj (or m_j), p_edge, rt ~ R_minus, delta(rt), Uw(rt)
Set tolerances eps_p, eps_m, eps_L and iteration limits

repeat (outer nonlinear loop)
  # 1) Wall-jet integration (requires jet init and pedestal pressure)
  compute m_j = rho * Uj * b0
  set q(rt) = m_j / (2*pi*rt*rho)
  set m(rt) = m_j * Uj / (2*pi*rt)
  integrate wall-jet ODEs for {q(r), m(r), delta(r)} from r=rt to R_max
    using correlations Cf(Re_delta) and growth d(delta)/dr
  from jet vertical momentum, infer pedestal pressure profile p_ped(r)
    such that momentum turning is satisfied and matches wall-jet m(r)
  evaluate p_edge_candidate = p0 + p_ped(R_minus)

  # 2) Core thin-film solve with edge pressure
  solve lubrication equation for p_c(r) on [0, R_minus] with:
    dp_c/dr|_{r=0}=0 and p_c(R_minus)=p_edge_candidate
  compute leakage: m_leak = 2*pi*R_minus*rho*h*ubar(R_minus)
    where ubar = -(h^2/(12*mu))*dp_c/dr

  # 3) Global constraints and updates
  residuals:
    R_p = p_edge - p_edge_candidate
    R_m = m_in - (m_j + m_leak)
    R_L = (integral_0^{R-} (p_c-p0) 2*pi*r dr) - W

  if max(|R_p|, |R_m|, |R_L|) < tolerances -> CONVERGED

  # 4) Nonlinear update (quasi-Newton / fixed-point mix)
  update (Uj, p_edge, rt) using a 3x3 Jacobian-free secant step
    e.g., Broyden update with line search to reduce residual norm
  optionally under-relax delta- and Cf-related profiles if needed

until converged or iteration limit reached
post-process: fields {p_c, ubar, q, m, delta}, metrics {L(h), Wdot_jet, Pi_seal,
    ↪ Pi_leak, eta}
```

Complexity and robustness. The core solve is a banded linear system $\mathcal{O}(N)$. The wall-jet step is $\mathcal{O}(M)$ with M radial steps from r_t to $R_{\max}$. The outer Broyden loop typically converges in ∼5–15 iterations for practical tolerances. Under-relaxation of $(U_j, p_{\text{edge}}, r_t)$ and slope limiting on $\delta(r)$ improve robustness at high Reynolds numbers.

6 Governing Equations (compact summary)

For quick reference, the model equations are:

Core: $$\bar{u} = -\frac{h^2}{12\mu}\frac{dp_c}{dr}, \quad \frac{1}{r}\frac{d}{dr}(r\,\rho h\bar{u}) = s(r), \quad L = \int_0^{R^-}(p_c - p_0)2\pi r\,dr = W.$$

Jet: $$\dot{m}_j = \rho U_j b_0, \quad \dot{m}_j U_j = \int_{r_t^-}^{r_t^+}(p_{\text{ped}} - p_0)\,dr + \Delta\mathcal{M}_z.$$

Wall-jet: $$\frac{d}{dr}(\rho q) = 2\pi r \rho E U_w, \quad \frac{d}{dr}(\rho m) = -\tau_w 2\pi r - \frac{dp}{dr}2\pi r\delta, \quad \tau_w = \tfrac{1}{2}\rho C_f U_w^2.$$

Coupling: $$p_c(R^-) = p_0 + p_{\text{ped}}(R^-), \quad \dot{m}_{\text{leak}} = 2\pi R^- \rho h\bar{u}(R^-), \quad \dot{m}_{\text{in}} = \dot{m}_j + \dot{m}_{\text{leak}}.$$

7 Simulation Outputs

The results produced from the model are shown in this section. Unless otherwise noted, fields are reported in non-dimensional form with the jet speed and slot width as reference scales.

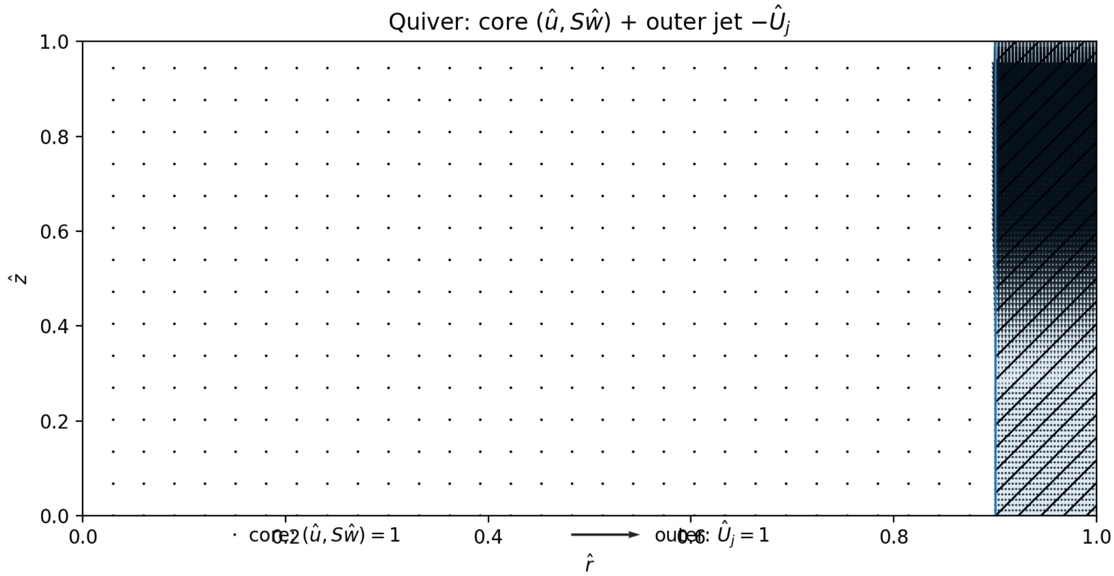

Figure 2 – Non-dimensional velocity field (quiver). Vectors show $(\hat{u}, S\hat{w})$ for isotropic visual scaling; the pattern reflects the pedestal pressure induced by the turning jet.

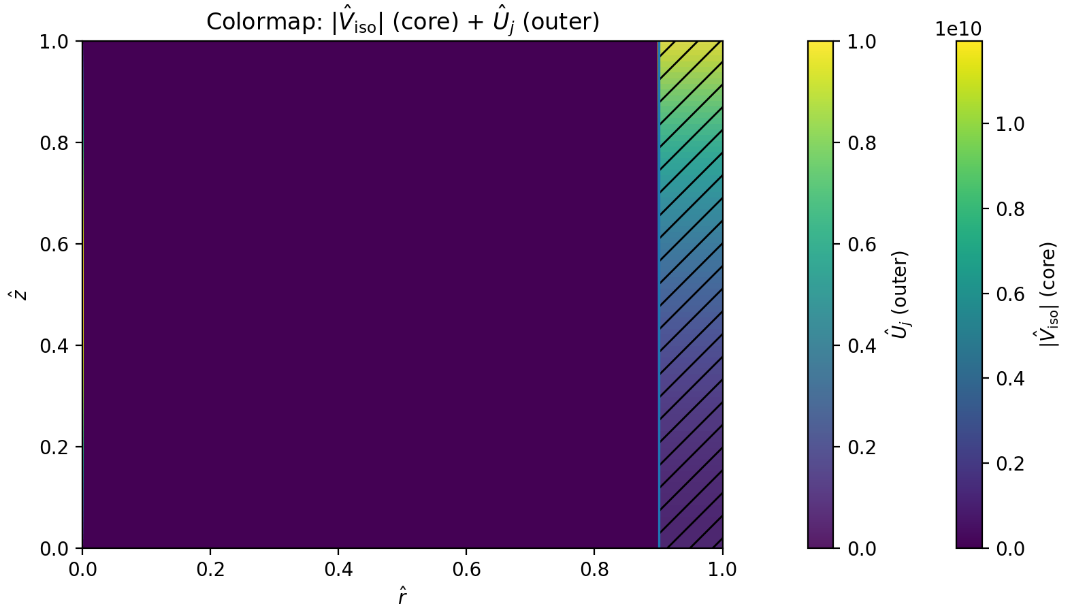

Figure 3 – Colormap of the non-dimensional isotropic speed magnitude $\hat{V}_{\rm iso} = \sqrt{\hat{u}^{\,2} + S^2 \hat{w}^{\,2}}$.

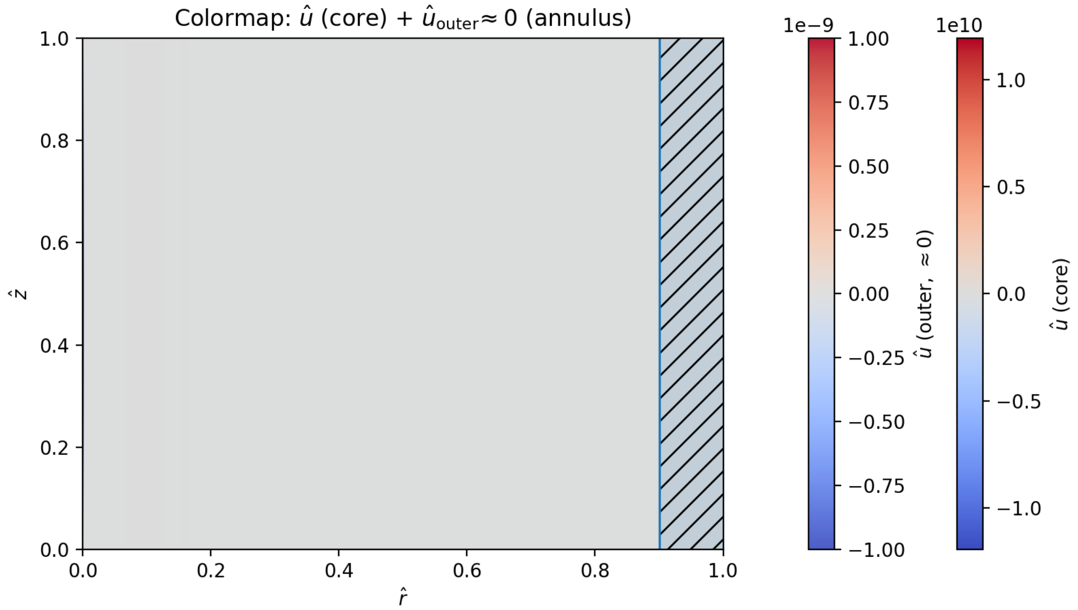

Figure 4 – Colormap of the non-dimensional radial component magnitude $|\hat{u}|$.

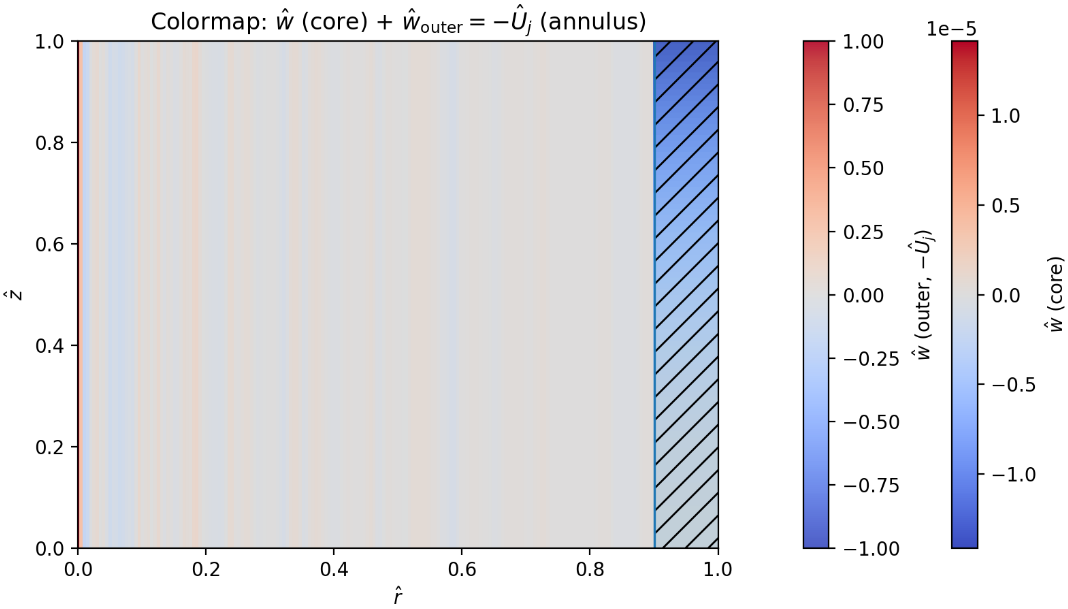

Figure 5 – Colormap of the non-dimensional axial component magnitude $|\hat{w}|$.

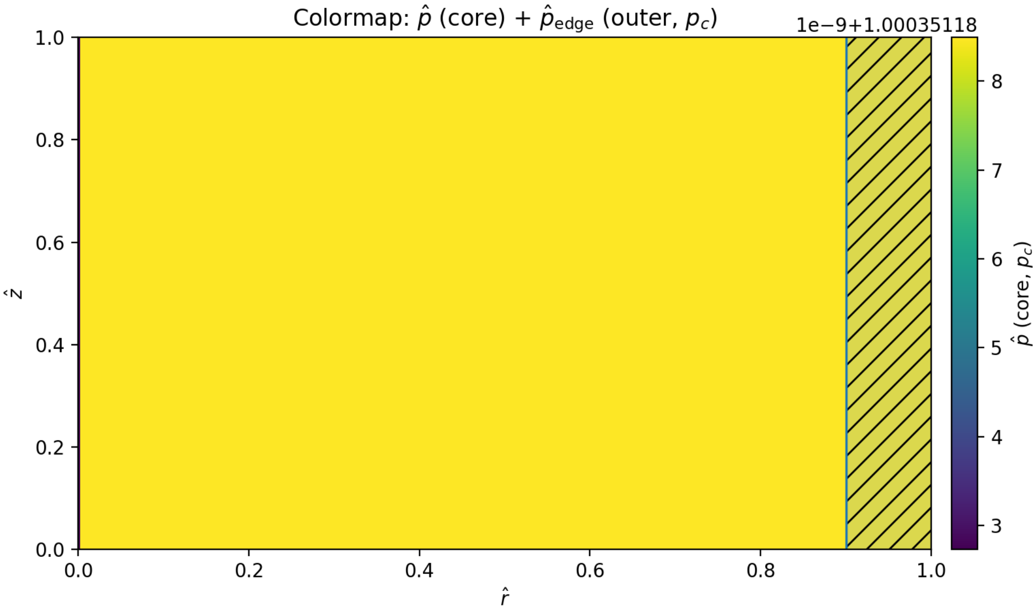

Figure 6 – Colormap of the non-dimensional pressure $\hat{p}$.

Performance and stability analysis. From the converged solutions the lift–height characteristic $L(h)$ is evaluated to assess static stability. A stable hovering point satisfies $dL/dh < 0$ near the nominal gap. The required jet power is estimated as

$$\dot{W}_{\text{jet}} = \frac{1}{2}\dot{m}_{\text{out}}U_{\text{out}}^2/(1 + K_{\text{turn}}), \tag{12}$$

and the non-dimensional sealing and leakage indices are

$$\Pi_{\text{seal}} = \frac{\rho_j U_{\text{out}}^2 b_0}{h\,\overline{p_c}}, \qquad \Pi_{\text{leak}} = \frac{\dot{m}_{\text{leak}}}{\rho U_{\text{out}} 2\pi R^- b_0}. \tag{13}$$

Together with the seal number Σ and the efficiency $\eta = \dfrac{Wh}{\dot{W}_{\text{jet}}}$, these provide compact performance metrics for design optimization.

8 Discussion

This momentum-based framework determines the sealing pressure and lift directly from the interplay between the impinging jet and the confined core flow. The approach ensures that the sealing effect arises as a natural consequence of conservation laws, with only standard, measurable correlations in the wall-jet closure.

9 Conclusions

We have formulated a self-consistent, momentum-driven description of jet-induced sealing flows. The model couples lubrication pressure in the core with integral balances in the jet and wall-jet regions, and provides an implementable numerical algorithm with clear convergence criteria. All relevant physical quantities emerge from conservation principles, offering a transparent basis for prediction and design.